

Atomistic simulations of oxide ion diffusion in heavily doped lanthanum cobaltite

C.A.J. Fisher^{a,*}, Y. Iwamoto^a, M. Asanuma^b, T. Anyashiki^b, K. Yabuta^c

^a Japan Fine Ceramics Center, 2-4-1 Mutsuno, Atsuta-ku, Nagoya 456-8587, Japan

^b JFE Steel, 1 Kokan-cho, Fukuyama, Hiroshima 721-8510, Japan

^c JFE Steel, 1-1 Minami-watarida-cho, Kawasaki-ku, Kawasaki 210-0855, Japan

Received 21 April 2004; received in revised form 27 July 2004; accepted 29 July 2004

Available online 29 September 2004

Abstract

Molecular dynamics simulations of perovskite-structured LaCoO_3 doped with alkaline earth and transition metal elements have been performed to provide a theoretical assessment of the relationship between oxide ion conductivity and composition in this system. Conductivities for compositions $\text{La}_{1-x}\text{Sr}_x\text{Co}_{1-y}\text{Fe}_y\text{O}_{3-\delta}$ ($0.8 < x < 0.9$, $0 < y < 1.0$) at 1500°C are reported. Several compositions are simulated at other temperatures in order to estimate the activation energies for ionic conductivity. Conductivity is found to increase with increasing strontium content, but exhibits a minimum for iron contents of 50% irrespective of the strontium content. Although substitution of Co^{2+} ions for Co^{3+} ions increases the volume fraction of oxide ion vacancies, the ionic conductivity decreases as a result of strong interactions between the lower valency dopants and vacancies.

© 2004 Elsevier Ltd. All rights reserved.

Keywords: Ionic conductivity; Perovskites; Membranes; Molecular dynamics; LaCoO_3

1. Introduction

Mixed oxide ionic and electronic conductors find use in a number of electrochemical applications such as electrodes (for batteries and ceramic fuel cells), separation membranes (for generating high purity oxygen gas), and automotive and industrial catalysts.¹ The system $\text{La}_{1-x}\text{Sr}_x\text{Co}_{1-y}\text{Fe}_y\text{O}_{3-\delta}$ (LSCF) exhibits unusually high oxide ion conductivity and good electronic conductivity over a wide range of dopant concentrations, and has been the focus of many studies in recent years.^{2–7} The phase relations in this system, however, are complex^{8,9} and depend strongly not only on the composition, but also on the synthesis and test conditions. The crystal structures of the end members are known to vary with temperature (Fig. 1), atmosphere and thermal his-

tory, as do the charges of the transition metal ions and enthalpies of oxygen vacancy formation.^{7,8} In general, however, all compositions tend towards a disordered oxygen vacancy cubic perovskite ($\text{ABO}_{3-\delta}$) structure at elevated temperatures (typically $> 900^\circ\text{C}$). Higher La and Fe contents are known to stabilize the perovskite structure down to lower temperatures.¹⁰ The stability of the material and suppression or removal of phase transformations are important considerations, particularly when preparing gas-tight components that are subjected to variable temperatures during service.

Computer simulation can provide useful insights into oxide ion diffusion since this phenomenon is difficult to probe at the atomic level by experimental techniques. Islam et al.^{11–14} have performed a number of simulations of doped LaMO_3 perovskites ($M = \text{Mn}^{3+}$, Co^{3+} , Cr^{3+} , Fe^{3+}) using a combination of static lattice (SL) and molecular dynamics (MD) methods. They showed that anion vacancy formation is favoured over hole formation (assuming typical oxygen partial pressures) when doping with aliovalent ions¹³ and

* Corresponding author. Present address: Materials Chemistry Group, Chemistry Division, University of Surrey, Guildford GU2 7XH, UK. Tel.: +44 1483 689591; fax: +44 1483 686851.

E-mail address: c.a.j.fisher@surrey.ac.uk (C.A.J. Fisher).

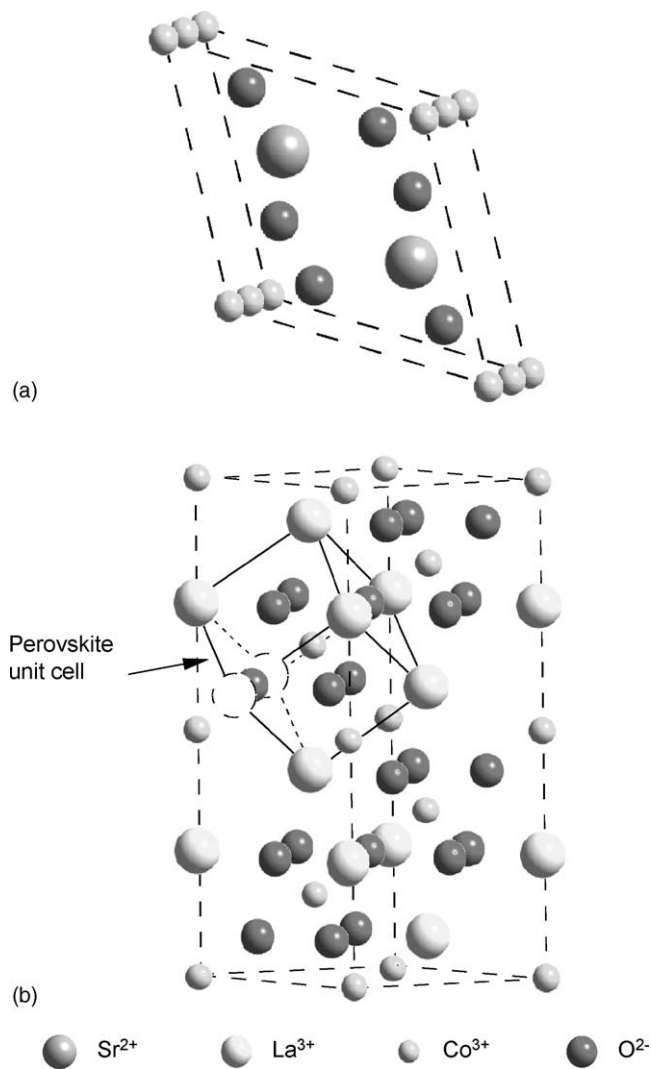


Fig. 1. The room temperature unit cell structures of (a) SrCoO_3 (hexagonal, S.G. $P6_3mc$) and (b) LaCoO_3 (rhombohedral, S.G. $R3m$). The relationship between the perovskite structure (shared by LaFeO_3 and SrFeO_3) and the rhombohedral cell of LaCoO_3 is also shown.

that $\text{La}_{0.8}\text{Sr}_{0.2}\text{CoO}_{3-\delta}$ is a better oxide ion conductor than $\text{La}_{0.8}\text{Sr}_{0.2}\text{MnO}_{3-\delta}$.¹⁴ However, they have generally confined their studies to dopant contents $\leq 20\%$. In this paper we report results for MD simulations of compositions near the end member $\text{SrCoO}_{3-\delta}$, and examine the effect of iron content on oxide ion diffusion. To examine the influence of oxidation states on ionic conductivity, we simulated a number of compositions with transition metal ions in a mixture of +2 and +3 charge states.

2. Simulation method

The MOLDY code¹⁵ was used for all simulations. Interactions between ions were described by an empirical potential in which the forces are divided into a long-range Coulombic term (calculated by Ewald Summation) and a short-range

term of the Buckingham form:

$$\phi_{ij}(r) = A_{ij} \exp\left(-\frac{r}{\rho_{ij}}\right) - \frac{C_{ij}}{r^6}$$

where ϕ_{ij} is the potential energy between ions i and j separated by distance r , and A_{ij} , ρ_{ij} and C_{ij} are potential parameters particular to each ion pair. We used the parameters of Read et al.¹³ combined with those of Lewis and Catlow¹⁶ as these successfully reproduce the perovskite crystal structure and elastic constants even when all particles are treated as rigid ions.

We first performed simulations of 22 compositions, namely $\text{La}_{1-x}\text{Sr}_x\text{Co}_{1-y}\text{Fe}_y\text{O}_{3-\delta}$ with $x = 0.8$ or 0.9 and $y = 0, 0.1, 0.2, 0.3, 0.4, 0.5, 0.6, 0.7, 0.8, 0.9$ or 1.0 , assuming charges of +3 for both cobalt and iron ions. (Hereafter we refer to the various compositions in terms of the stoichiometric ratios of their component cations, so that $\text{La}_{0.2}\text{Sr}_{0.8}\text{Co}_{0.8}\text{Fe}_{0.2}\text{O}_{2.6}$ is called LSCF2882 and so on.) For these compositions the number of oxygen vacancies depends on the amount of Sr^{2+} only. Iodometric titration measurements of oxygen contents in the strontium end member system have shown that cobalt typically exists in a lower oxidation state than iron.^{16,17} We therefore also performed simulations for a small number of compositions with the charge of the cobalt ions reduced to 2+ (and the corresponding number of oxygen ions removed to maintain charge neutrality). The difficulty of generating reliable potentials for Co^{4+} or Fe^{4+} , and the lack of such potentials in the literature, precluded us from including a study of Co(IV)/Fe(IV) -containing systems. However, Mizusaki et al.¹⁸ have shown that the oxygen deficiency, δ , in $\text{La}_{1-x}\text{Sr}_x\text{CoO}_{3-\delta}$ increases rapidly with temperature and x , even in oxygen atmospheres, so that our assumption of negligible Co(IV)/Fe(IV) content is not unrealistic.

The cubic perovskite structure was assumed for all compositions, with Sr and Fe ions distributed randomly over A and B sites, respectively. Simulation boxes, constructed from $8 \times 8 \times 8$ perovskite unit cells and containing around 2400 atoms, were equilibrated at 1500°C and 0.1 MPa for over 20,000 time steps, with 1 step = 2 fs, until a constant average internal energy was obtained. The simulation box was then held fixed at the average equilibrated volume, and further equilibrated for 5000 steps in the canonical (constant volume–constant temperature) ensemble. Simulation production runs of 60,000 time steps were commenced from this equilibrated structure. Simulations were also performed in an identical manner at 1000, 1400 and 1700°C for several compositions with all B-site ions in the +3 state to estimate the oxide ion migration enthalpy, ΔH_m , from an Arrhenius plot of $\ln(\sigma T)$ versus inverse temperature.

Oxygen ion conductivities, $\sigma_{\text{O}^{2-}}$, were calculated using the Nernst–Einstein equation with diffusion coefficients obtained from plots of mean square displacement (msd) versus time. A correlation factor of 0.69 was used for the perovskite structure.¹⁹ As the initial part of an msd versus time plot typically does not correspond to the long-range diffusive behavior

(and is usually curved as a result), the gradient was calculated from the (straight) section in the latter half (30–60 ps) of each plot.

Although cation ordering is a possibility in the heavily doped materials, the lack of experimental evidence for this in the current system means that a random distribution of cations is a reasonable model to use at this stage. The distribution of the dopant cations, however does have a significant effect on the ionic conductivity, as will be discussed below, resulting in a relatively large uncertainty in the values obtained. To quantify this uncertainty, three compositions (LSCF1955, LSCF1964 and LSCF2855) were simulated using three different random dopant distributions, and the average value and standard deviations of the ionic conductivities calculated.

3. Results and discussion

Fig. 2 shows a plot of the cubic lattice parameter of each composition as a function of iron content at 1500 °C. The crystal volume increases with increasing Sr^{2+} content, as a consequence of the larger size of the Sr^{2+} ion, as has been observed experimentally by Petrov et al.⁸ Increasing the iron content also expands the crystal structure, consistent with the slightly larger ionic radius of Fe(III) compared to Co(III).²⁰ It is interesting to note that there appears to be a change of slope between $y = 0.6$ and 0.7 (most notably for $x = 0.9$). Ten Elshof and Boeijmsma²⁰ observed a decrease in slope of the pseudo-cubic parameter in $\text{La}_{0.6}\text{Sr}_{0.4}\text{Co}_{1-y}\text{Fe}_y\text{O}_{3-\delta}$ below $y = 0.4$, which they attributed to changes in ionic charge. As the charges in our simulation are constant, the change in slope of the calculated lattice parameters must have a different cause, one that is most likely connected with geometric factors, such as the distribution and number of nearest neighbouring B-site dopants.

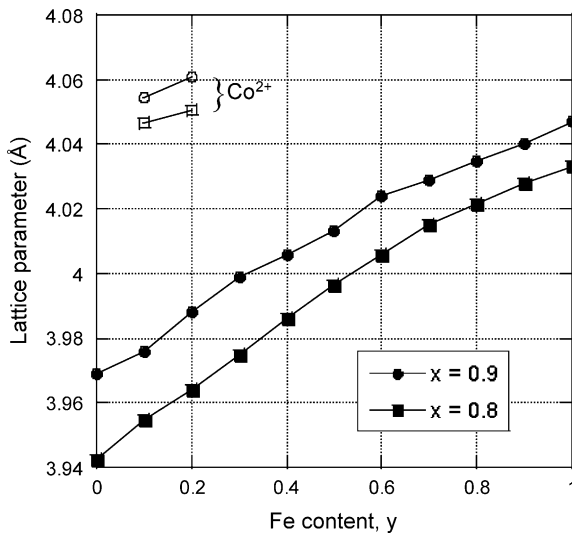


Fig. 2. Lattice parameters vs. iron content for all compositions $\text{La}_{1-x}\text{Sr}_x\text{Co}_{1-y}\text{Fe}_y\text{O}_{3-\delta}$, including those containing Co^{2+} , at 1500 °C.

When lower valence cobalt ions were introduced, the lattice expanded further because of the larger size of the 2+ ions compared to their 3+ counterparts. Increasing the divalent cation content results in an increased number of O^{2-} vacancies, which tends to make the lattice contract. The interplay between these two competing tendencies can explain the slight increase in lattice parameter on reducing the Co^{2+} content and increasing the Fe^{3+} content, i.e., the increase in the number of O^{2-} ions slightly outweighs the effect of the decrease in ionic radius at these concentrations.

The average temperature calculated during the course of the production runs was within ± 20 °C of the target temperature of 1500 °C for all compositions, indicating that the structures were reasonably well equilibrated. Calculation of the average lattice parameters for the three compositions simulated with different ion distributions found the standard deviation to be between 0.001 and 0.02%. These very small values indicate that the perovskite unit cell of each composition did not vary significantly between the different (random) distributions.

A typical plot of msd versus time is shown in Fig. 3 for LCSF2882. Beyond the initial short-range region, the oxygen msd increases linearly with time, indicating fast ion diffusion has occurred. As expected, no cation diffusion was observed due both to the short time scale of the simulation and the absence of defects on the cation sublattice. However, $\text{Co}^{2+/3+}$ ions did show a small increase in msd with time (smaller than the average interatomic spacing), which was found to result from the ions “rattling around” their ideal (B site) positions within their octahedral cages. This positional instability is likely related to the distortions of the perovskite structure and phase transformations observed in actual LaCoO_3 and SrCoO_3 specimens.

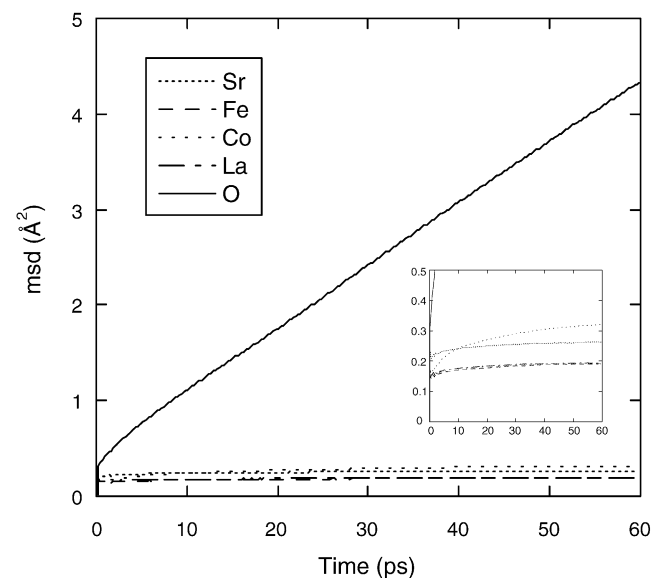


Fig. 3. Mean square displacement as a function of time for $\text{La}_{0.2}\text{Sr}_{0.8}\text{Co}_{0.8}\text{Fe}_{0.2}\text{O}_{2.6}$ at 1500 °C. The inset shows a magnified view of the cation msds.

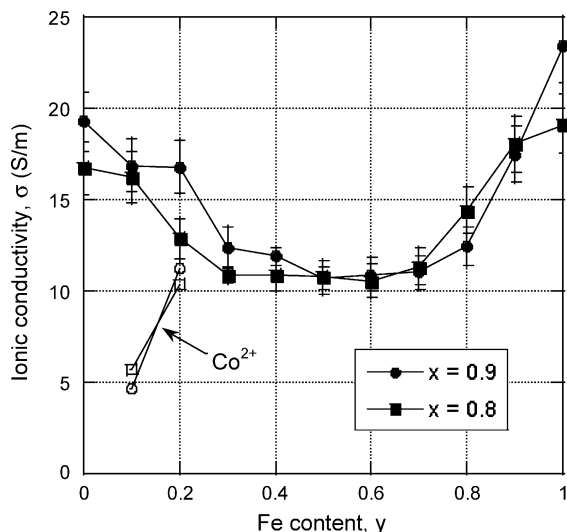


Fig. 4. Oxide ion conductivity vs. iron content for all compositions $\text{La}_{1-x}\text{Sr}_x\text{Co}_{1-y}\text{Fe}_y\text{O}_{3-\delta}$, including those containing Co^{2+} , at 1500 °C.

The oxide ion conductivities, $\sigma_{\text{O}^{2-}}$, of each composition are plotted as a function of iron content in Fig. 4. As has been found in simulations of other highly disordered systems, such as yttria-stabilized zirconia,²¹ the conductivities calculated were strongly dependent on the dopant distribution. This is a consequence of the small size (relative to real, macroscopic materials) of the simulation box, so that any clustering of a particular species has a disproportionately large trapping effect on the oxide ions.

Simulations with dopants randomly substituted on different sites produced standard deviations of 8.6% in the case of LSCF1955 and 3.8% in the case of LSCF1964. We have taken this larger value to be the uncertainty for compositions simulated from only one starting configuration, and plotted these as error bars in Fig. 4. Conductivities could therefore vary by as much as ± 2.0 S/m in the higher conductivity compositions, although this is likely to be an overestimate.

Despite the large uncertainties associated with each conductivity, some overall trends can be discerned. For systems containing Co^{3+} and Fe^{3+} only, the conductivity decreases with increasing iron content to a minimum near $y = 0.5$. This trend is consistent with impedance measurements using blocking electrodes of compositions LSCF2891 and LSCF2882 at 900 °C.²² However, the same study found that the oxygen permeability of iron-free composition LSC19 was lower than that of both LSCF2891 and LSCF2882, while our simulation results predicted it to be higher. This disparity is thought to be due to the fact that, unlike the iron-doped samples, LSC19 undergoes a phase transformation at intermediate temperatures from the hexagonal to perovskite structure which compromises the integrity of the sample due to the large volume changes involved;²² any residual hexagonal phase will also decrease the oxygen flux. The increase in ionic conductivity with increased strontium content is consistent with experimental results reported by Ten Elshof et al.⁶

and can be explained by the increased number of vacancies formed on increasing the number of lower valence ions.

As the Fe^{3+} content is increased beyond $y = 0.5$, the oxide ion conductivity increases to a maximum at $y = 1.0$. Below $y = 0.5$, Fe is the minority species with Co constituting the matrix; above $y = 0.5$, Co becomes the minority species, while the matrix consists of Fe ions. Using the Gulp code²³ to perform static lattice simulations, we found that a slight binding force is exerted by a dopant Fe^{3+} ion on an oxygen vacancy in a matrix of Co^{3+} ions, with the vacancy most stable at a next-nearest neighbour position. Similarly, an isolated Co^{3+} ion in LaFeO_3 is bound more strongly to an oxygen vacancy than the Fe^{3+} matrix ions. We therefore attribute this parabolic-like variation in conductivity to a mixing effect in which pairs and triplets of dopants, which result in very strong dopant-vacancy interactions, are a maximum at $y = 0.5$. Expressing this idea in a slightly different way, we can say that the energy surface encountered by migrating oxide ions is essentially homogeneous in all three directions in the undoped (end member) compositions, which is conducive to rapid ion diffusion. The most uneven energy surface is encountered when Co:Fe ratio is 50:50, resulting in a minimum in conductivity.

When the B-site cation is reduced to the 2+ state, the ionic conductivity decreases further, despite the larger number of oxide ion vacancies that are formed (to maintain charge balance). This can be attributed to the strong attractive force between the vacancies (effective positive charge) and lower valency dopants (effective negative charge), which traps the vacancies. This effect was most noticeable in compounds $\text{La}_{1-x}\text{Sr}_x\text{Co}_{0.9}\text{Fe}_{0.1}\text{O}_{2.55}$, where $x = 0.8$ or 0.9, which exhibited the lowest conductivities of the compositions examined in this study. Increasing the iron content dramatically increased the ionic conductivity as the proportion of strongly vacancy-binding Co^{2+} defects was reduced. In real systems, it is possible that redox transfer between divalent and trivalent cations, in concert with oxide ion diffusion, reduces the migration barrier; unfortunately this complex phenomenon is beyond the scope of our purely ionic model. Experimental evidence suggests, however, that the oxidation state of cobalt is closer to +2.5 than +2, so that our compositions represent “extreme” cases in which the trapping forces are stronger than in the real material. Furthermore, the oxidation state of iron has been measured to be slightly greater than 3+, so that in real materials the increase in oxide ion conductivity for iron contents above $y = 0.5$ may be more subdued, as the number of oxygen vacancies will also decrease. In the case of high cobalt content, high vacancy fractions and low oxidation states can be expected to lead to ordering of anion vacancies (e.g., to give a brownmillerite structure⁷), particularly at low temperatures and low oxygen partial pressures, resulting in an even lower overall ionic conductivity.

From the plot of conductivity against inverse temperature shown in Fig. 5, we estimate the migration enthalpy for oxide ion diffusion to be between 0.7 eV and 1.0 eV, slightly greater than the values of 0.5–0.6 eV calculated by Islam et

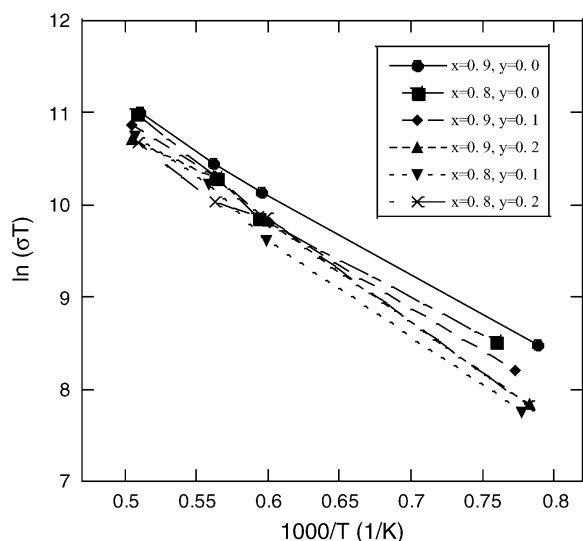


Fig. 5. Arrhenius plots of oxide ion conductivity times temperature vs. inverse temperature for compositions $\text{La}_{1-x}\text{Sr}_x\text{Co}_{1-y}\text{Fe}_y\text{O}_{3-\delta}$, with both Co and Fe in the trivalent state.

al.¹⁴ for $\text{La}_{1-x}\text{Sr}_x\text{CoO}_{3-\delta}$ ($x = 0.1, 0.2$) using a different set of potentials. The activation energy also appears to increase slightly with increasing iron content, although a larger number of compositions need to be simulated at different temperatures for this to be confirmed. Our diffusion coefficients and conductivities are the same order of magnitude as those calculated by Islam et al.¹⁴ and compare well with experimental values reported by Carter et al.²⁴ for $\text{La}_{1-x}\text{Sr}_x\text{CoO}_{3-\delta}$.

Although $\text{La}_{0.1}\text{Sr}_{0.9}\text{Co}_{0.255}\text{O}_{2.55}$ shows the highest conductivity in our simulations, in practice its crystal structure transforms from cubic perovskite to hexagonal (2H-BaNiO₃) symmetry as the temperature is lowered; the large volume changes associated with this make it unsuitable for use as a dense ceramic membrane. Of the compositions known to retain the perovskite structure to room temperature, $\text{La}_{0.1}\text{Sr}_{0.9}\text{Co}_{0.9}\text{Fe}_{0.1}\text{O}_{2.55}$ has the lowest activation energy and highest conductivity of the compositions examined here, and thus is considered to be the most suitable material for use as an oxygen separator membrane.

4. Conclusion

The oxide ion conductivities, $\sigma_{\text{O}^{2-}}$, of 26 compositions in the system $\text{La}_{1-x}\text{Sr}_x\text{Co}_{1-y}\text{Fe}_y\text{O}_{3-\delta}$ ($0.8 < x < 0.9$, $0 < y < 1.0$) at 1500°C have been calculated from MD simulations. The fraction of vacancies and the amount and charge of the transition metal ions were found to have a large effect on $\sigma_{\text{O}^{2-}}$. Although $\text{La}_{0.1}\text{Sr}_{0.9}\text{Co}_{0.255}\text{O}_{2.55}$ displayed the highest conductivity in the present study, its structural transformation at lower temperatures makes it unsuitable for use as a dense separation membrane. $\text{La}_{0.1}\text{Sr}_{0.9}\text{Co}_{0.9}\text{Fe}_{0.1}\text{O}_{2.55}$ is therefore considered the most promising material (of the compositions examined here) for this application.

Acknowledgements

This work was carried out as part of the Coke Oven Gas (COG) project of the Japan R&D Center for Metals (JRCM) with funding from the Ministry of Economy, Trade and Industry (METI), Japan.

References

1. Kharton, V. V., Naumovich, E. N. and Nikolaev, A. V., Materials of high-temperature electrochemical oxygen membranes. *J. Membr. Sci.*, 1996, **111**, 149–157.
2. Mineshige, A., Kobune, M., Fujii, S., Ogumi, Z., Inaba, M., Yao, T. et al., Metal-insulator transition and crystal structure of $\text{La}_{1-x}\text{Sr}_x\text{CoO}_3$ as a function of Sr-content, temperature and oxygen partial pressure. *J. Solid State Chem.*, 1999, **142**, 374–381.
3. Chen, C.-S., Zhang, Z.-P., Jiang, G. S., Fan, C.-G., Liu, W. and Bouwmeester, H. J. M., Oxygen permeation through $\text{La}_{0.4}\text{Sr}_{0.6}\text{Co}_{0.2}\text{Fe}_{0.8}\text{O}_{3-\delta}$ membrane. *Chem. Mater.*, 2001, **13**, 2797–2800.
4. Scott, S. P., Mantzavinos, D., Hartley, A., Sahibzada, M. and Metcalfe, I. S., Reactivity of LSCF perovskites. *Solid State Ionics*, 2002, **152/153**, 777–781.
5. Wang, S., van der Heide, P. A. W., Chavez, C., Jacobson, A. J. and Adler, S. B., An electrical conductivity relaxation study of $\text{La}_{0.6}\text{Sr}_{0.4}\text{Fe}_{0.8}\text{Co}_{0.2}\text{O}_{3-\delta}$. *Solid State Ionics*, 2003, **156**, 201–208.
6. Ten Elshof, J. E., Lankhurst, M. H. R. and Bouwmeester, H. J. M., Oxygen exchange and diffusion coefficients of strontium-doped lanthanum ferrites by electrical conductivity relaxation. *J. Electrochem. Soc.*, 1997, **144**, 1060–1067.
7. Ten Elshof, J. E., Bouwmeester, H. J. M. and Verweij, H., Oxygen transport through $\text{La}_{1-x}\text{Sr}_x\text{FeO}_3$ membranes. I. Permeation in air/He gradients. *Solid State Ionics*, 1995, **81**, 97–109.
8. Petrov, A. N., Kononchuk, O. F., Andreev, A. V., Cherepanov, V. A. and Kofstad, P., Crystal structure, electrical and magnetic properties of $\text{La}_{1-x}\text{Sr}_x\text{CoO}_{3-y}$. *Solid State Ionics*, 1995, **80**, 189–199.
9. Vashook, V. V., Zinkevich, M. V. and Zonov, Yu. G., Phase relations in oxygen-deficient $\text{SrCoO}_{2.5-\delta}$. *Solid State Ionics*, 1999, **116**, 129–138.
10. Teraoka, Y., Zhang, H.-M. and Furukawa, S., Oxygen permeation through perovskite-type oxides. *Lett. Chem. Soc. Jpn.*, 1985, **11**, 1743–1746.
11. Islam, M. S., Cherry, M. and Winch, L. J., Defect chemistry of LaBO_3 (B = Al, Mn or Co) perovskite-type oxides. *J. Chem. Soc., Faraday Trans.*, 1996, **92**, 479–482.
12. Cherry, M., Islam, M. S. and Catlow, C. R. A., Oxygen ion migration in perovskite-type oxides. *J. Solid State Chem.*, 1995, **118**, 125–132.
13. Read, M. S. D., Islam, M. S., Watson, G. W., King, F. and Hancock, F. E., Defect chemistry and surface properties of LaCoO_3 . *J. Mater. Chem.*, 2000, **10**, 2298–2305.
14. Islam, M. S., Cherry, M. and Catlow, C. R. A., Oxygen diffusion in LaMnO_3 and LaCoO_3 perovskite-type oxides: a molecular dynamics study. *J. Solid State Chem.*, 1996, **124**, 230–237.
15. Refson, K. D., Moldy: a portable molecular dynamics simulation program for serial and parallel computers. *Comput. Phys. Commun.*, 2000, **126**, 309–328.
16. Lewis, G. V. and Catlow, C. R. A., Potential models for ionic oxides. *J. Phys. C: Solid State Phys.*, 1985, **18**, 1149–1161.
17. Kokhanovskii, L. V., Vashuk, V. V., Vil'kotskaya, E. F., Vitushko, S. I. and Zinkevich, M. V., Synthesis, structure, and some physicochemical properties of $\text{SrCo}_{1-x}\text{Fe}_x\text{O}_{3-d}$. *Inorg. Mater.*, 1999, **35**, 282–286.
18. Mizusaki, J., Mima, Y., Yamauchi, S. and Fueki, K., Nonstoichiometry of the perovskite-type oxides $\text{La}_{1-x}\text{Sr}_x\text{CoO}_{3-\delta}$. *J. Solid State Chem.*, 1989, **80**, 102–111.

19. Ishigaki, T., Yamauchi, S., Kishio, K., Mizusaki, J. and Fueki, K., Diffusion of oxide ion vacancies in perovskite-type oxides. *J. Solid State Chem.*, 1988, **73**, 179–187.
20. Ten Elshof, J. E. and Boeijmsma, J., Influence of iron content on cell parameters of rhombohedral $\text{La}_{0.6}\text{Sr}_{0.4}\text{Co}_{1-y}\text{Fe}_y\text{O}_3$. *Powder Diffract.*, 1996, **11**, 240–245.
21. Yamamura, Y., Kawasaki, S. and Sakai, H., Molecular dynamics analysis of ionic conduction mechanism in yttria-stabilized zirconia. *Solid State Ionics*, 1999, **126**, 181–189.
22. “Technology for Generating Hydrogen from Steelmaking Process Gases”, Project Report for FY 2002. Japan R&D Center for Metals (JRCM), Tokyo, 2003 (in Japanese).
23. Gale, J. D., Gulp: a computer program for the symmetry-adapted simulation of solids. *J. Chem. Soc., Faraday Trans.*, 1997, **93**, 629–637.
24. Carter, S., Selcuk, A., Chater, R. J., Kajda, J., Kilner, J. and Steele, B. C. H., Oxygen transport in selected nonstoichiometric perovskite-type oxides. *Solid State Ionics*, 1992, 597–605.